Available online at www.sciencedirect.com
SCIENCE DIRECT®
PHYSICS LETTERS A
ELSEVIER
Physics Letters A 312 (2003) 348–354
www.elsevier.com/locate/pla

Vibrational resonance and vibrational propagation in excitable systems

E. Ullner [a], A. Zaikin [a], J. García-Ojalvo [b,c,*], R. Báscones [b], J. Kurths [a]

[a] *Institut für Physik, Potsdam Universität, Am Neuen Palais 10, D-14469 Potsdam, Germany*
[b] *Departament de Física i Enginyeria Nuclear, Universitat Politècnica de Catalunya, Colom 11, E-08222 Terrassa, Spain*
[c] *Center for Applied Mathematics, Cornell University, Ithaca, NY 14853, USA*

Received 5 December 2002; received in revised form 11 April 2003; accepted 14 April 2003

Communicated by C.R. Doering

Abstract

We report the occurrence of vibrational resonance in excitable systems. Namely, we show that an optimal amplitude of the high-frequency driving enhances the response of an excitable system to a low-frequency signal. The phenomenon is confirmed in an excitable electronic circuit and in the FitzHugh–Nagumo model. In this last case we also analyze the influence of additive noise and the interplay between stochastic and vibrational resonance. Additionally, we show that this effect can be extended to spatially extended excitable media, taking the form of an enhanced propagation of the low-frequency signal.

1. Introduction

Signal detection by nonlinear systems can be considerably affected by external influences. The most relevant example of this fact is stochastic resonance (SR), where the response of a nonlinear system to a weak deterministic signal is enhanced by external random fluctuations [1]. Initially reported in bistable systems [2], SR has been found in many models and even natural systems [3,4], including excitable media [5].

In bistable systems, it has been shown that the role of noise in improving the quality of signal detection can be played by other types of driving, such as a chaotic signal [6] or a high-frequency periodic force [7]. In the latter case, known as *vibrational resonance* (VR), the system is under the action of a two-frequency signal. Such bichromatic signals are pervasive in many different fields, including brain dynamics [8], where, for instance, bursting neurons may exhibit two widely different time scales, and telecommunications [9], where information carriers are usually high-frequency waves modulated by a low-frequency signal that encodes the data. Two-frequency signals are also of interest in several other fields, such as laser physics [10], acoustics [11], neuroscience [12], and physics of the ionosphere [13]. The beneficial role of high-frequency (ultrasonic) driving has already been reported as increased drug uptake by brain cells [14], acceleration of bone and muscle repairing [15], and resonantly enhanced biodegradation of micro-orga-

* Corresponding author.
E-mail address: jordi.g.ojalvo@upc.es (J. García-Ojalvo).

0375-9601/03/$ – see front matter
doi:10.1016/S0375-9601(03)00681-9

nisms [16]. Additionally, ultrasonic irradiation of two widely different frequencies has been seen to enhance cavitation yield [17].

In contrast to the investigations in bistable systems, in this Letter we analyze the effect of high-frequency forcing in signal detection by *excitable* systems, and demonstrate the occurrence of VR in excitable media. Excitable systems have only one stable fixed point, but perturbations above a certain threshold induce large excursions in phase space, which take the form of spikes of fixed shape. The duration of these excursions introduces an intrinsic time scale in the system. Excitable systems are naturally sensitive to external perturbations. By way of example, they exhibit a resonant response to external harmonic driving [18,19]. Here we establish that this response can also be enhanced by a second, higher frequency periodic driving. In essence, we show that for an optimal amplitude of the high-frequency forcing, signal processing at the low-frequency driving is enhanced. This result indicates that the role of noise in standard stochastic resonance in excitable systems can also be played by a monochromatic driving.

First, we show that VR occurs in a simple electronic circuit with excitable properties, and confirm this effect by numerical simulation of the paradigmatic FitzHugh–Nagumo (FHN) model in an excitable regime. Next we study the effect of noise on this phenomenon, concluding that SR in excitable systems can be controlled by high-frequency driving. Finally, we show that this effect can also be observed in spatially extended systems of coupled excitable oscillators, in the form of resonant vibrational propagation of a low-frequency signal through the system for an optimal high-frequency driving applied to all elements in the system. Again, this result parallels the constructive role of noise in signal propagation through nonlinear media, which has been substantially studied in recent years in excitable [20], bistable [21], and even monostable [22] systems. The present results show that similar enhanced propagation can be obtained by replacing the broadband noisy driving with a single-frequency signal.

2. Vibrational resonance in an excitable electronic circuit

In order to demonstrate the occurrence of VR in an excitable system, we have constructed a simple electronic circuit based on Chua's diode, which has been implemented with an operational amplifier (OA) taken from the integrated circuit TL082 (see Fig. 1). When the voltage that controls this OA is asymmetric the circuit becomes excitable [23].

The signals from two function generators operating at widely different frequencies (1 kHz/50 kHz) are added and introduced into the system through the 1 nF condenser, as shown in Fig. 1. We have analyzed the behavior of the circuit for increasing amplitudes of the high-frequency (HF) harmonic driving, while keeping the amplitude of the low-frequency (LF) signal component fixed. The results are plotted in Fig. 2 (left) in terms of the voltage drop at the 1 nF

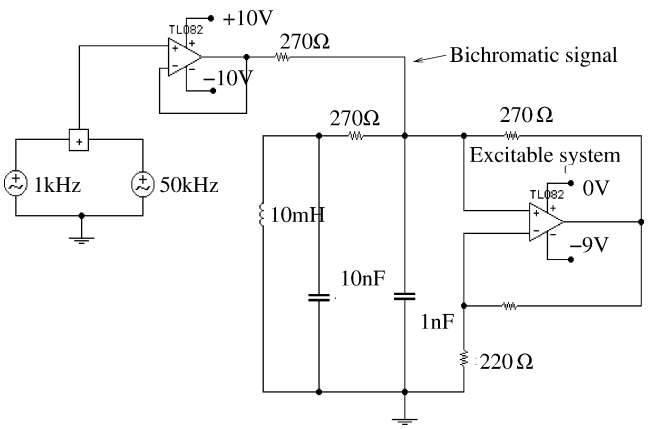

Fig. 1. Excitable electronic circuit exhibiting vibrational resonance.

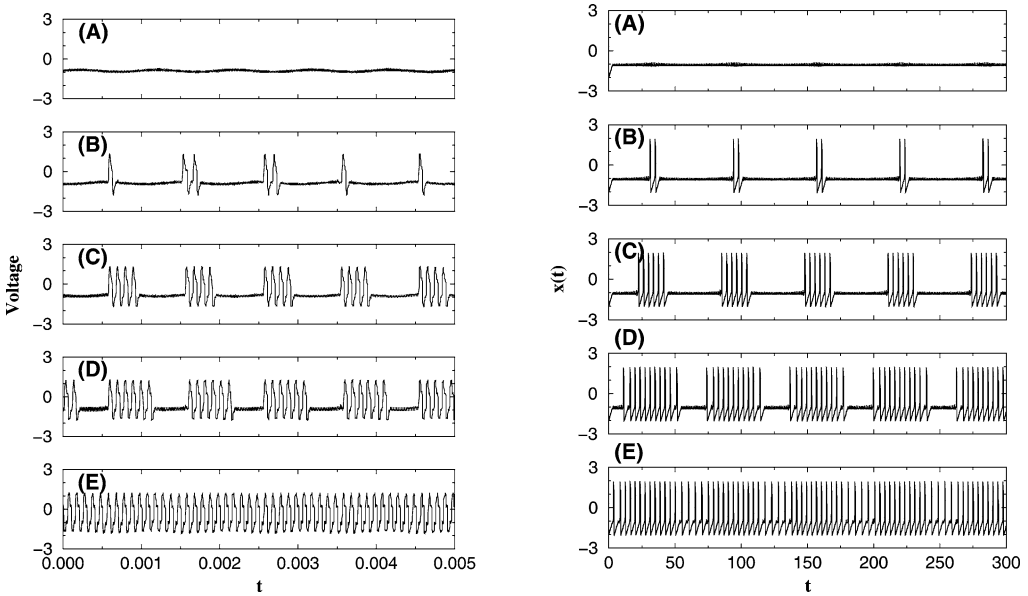

Fig. 2. Left: experimental results exhibiting vibrational resonance in the excitable electronic circuit of Fig. 1 under the action of a bichromatic signal. The voltage drop at the 1 nF condenser is plotted for different amplitudes of the high-frequency harmonic forcing: (A) 0.435 V, (B) 0.465 V, (C) 0.66 V, (D) 0.985 V, and (E) 1.385 V. The amplitude of the low-frequency component is fixed to 1.3 V. Right: corresponding regimes obtained by numerical simulations of the FitzHugh–Nagumo model for different HF amplitudes: (A) $B = 0.05$, (B) $B = 0.0505$, (C) $B = 0.055$, (D) $B = 0.065$, and (E) $B = 0.07$.

condenser. For a small enough amplitude of the HF component the total signal is below threshold, and hence there are no spikes in the system output, as shown in regime A of Fig. 2 (left). By increasing slightly the amplitude of the HF component, spikes start to appear at the low frequency (regime B). In this regime processing of the information (which is encoded in the LF signal) begins to occur, but can be considerably improved by further increasing the number of spikes per half period of the LF signal, since in this way the energy contained at this frequency is also increased. This happens in regimes C and D, which show the optimal detection of the LF signal. With further increase of the HF amplitude (regime E), the system fires immediately after reaching the stable point, so that the output mainly contains only the own frequency of the excitable system. Hence the LF component basically disappears from the system output, and signal processing is degraded again. This is a manifestation of vibrational resonance in an excitable medium, where an intermediate amplitude of a high-frequency driving leads to a resonant response at the low-frequency signal.

3. Vibrational resonance in the FitzHugh–Nagumo model

Next we show that the behavior reported in the previous section is not particular to the experimental system considered, but is a generic property of excitable systems. To that end we study numerically the FitzHugh–Nagumo (FHN) model, which is a paradigmatic model describing the behavior of firing spikes in neural activity [24], and in general the activator–inhibitor dynamics of excitable media [25]. In the presence of two harmonic signals, this model is defined by the following set of coupled equations:

$$\varepsilon \frac{dx}{dt} = x - \frac{x^3}{3} - y, \tag{1}$$

$$\frac{dy}{dt} = x + a + A\cos(\omega t) + B\cos(\Omega t) + \xi(t), \tag{2}$$

where $x(t)$ is the activator variable (representing the membrane potential in the neural case) and $y(t)$ is the inhibitor (related to the conductivity of the potassium channels existing in the neuron membrane [24]). The value of the time scale ratio $\varepsilon = 0.01$ is chosen so that

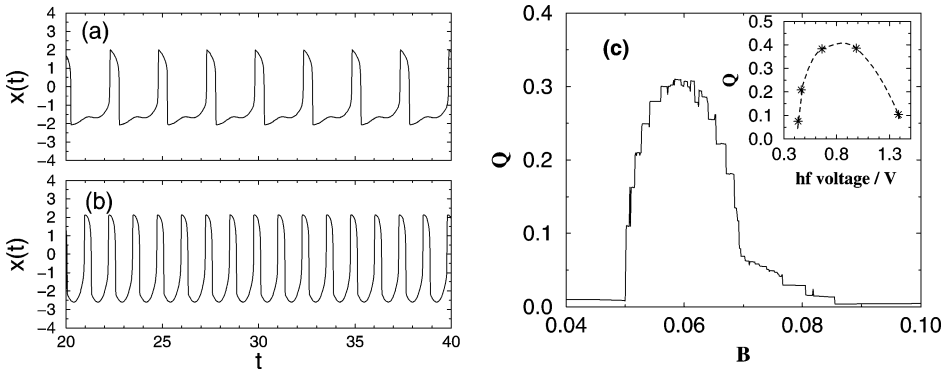

Fig. 3. (a) Oscillations exhibited by the bichromatically forced FHN model (1)–(2) at a frequency close to the own frequency of the system, and (b) at the driving high-frequency. The amplitude of the HF forcing is $B = 0.1$ and 10, respectively. (c) Response Q of the system at the low frequency ω vs. the amplitude B of the high-frequency input signal. The inset shows the corresponding figure for the electronic circuit results presented in Fig. 2 (left).

the activator evolves much faster than the inhibitor. Under these conditions the system is excitable for $a > 1$ [26]; we choose $a = 1.05$. $\xi(t)$ is a Gaussian white noise with zero mean and correlation $\langle \xi(t)\xi(t')\rangle = \sigma_a^2 \delta(t-t')$. The terms $A\cos(\omega t)$ and $B\cos(\Omega t)$ stand for the low- and high-frequency components of the external signal, respectively. In what follows we will chose $A = 0.01$, so that the system is below the excitation threshold (which is $A_{\text{thr}} \approx 0.075$ for $B = 0$), and $\Omega \gg \omega$, in particular $\Omega = 5$ and $\omega = 0.1$. In Eq. (2) we have considered no phase shift between the two driving signals, but it can be checked that the existence of an arbitrary phase shift does not alter the results that follow. To integrate model (1)–(2) we have used Heun's algorithm [27].

First we consider the noise-free case $\sigma_a = 0$ and, mimicking the electronic implementation described in the previous section, we fix the amplitude of the LF signal component and increase the HF amplitude. The different regimes exhibited by the FHN model under these conditions are shown in Fig. 2 (right). These regimes closely resemble the preceding observations made in the electronic circuit (compare left and right plots in the figure). As in that case, an increase of the HF amplitude B initially improves (regimes A–D) and finally degrades (regime E) signal processing at the low frequency, in what constitutes another case of vibrational resonance. Several additional aspects of the system behavior can be found in this model with respect to the electronic implementation. For instance, in regime E (Fig. 2 right) it is clearly seen that the intervals between spikes are not constant. This happens when the amplitude of the HF force is such that the system starts to fire asynchronously with respect to the signal. In this case, during one half of the signal period the system has to wait some time before spiking, whereas in the other half period the system can fire sooner once it reaches the stable point. This happens because in the latter case the time during which the signal is above threshold is larger, while the waiting time is close to the half period of the high-frequency force. Increasing the amplitude B further leads to a very regular spiking, as in the regime E of the electronic circuit (see also Fig. 3(a)). Finally, for large enough values of B we obtain a new regime that has not been observed in the circuit. In this regime, the oscillations happen with a frequency different from the own frequency of the system (i.e., the one related to the intrinsic time scale of the spiking behavior), but correspond in fact to the high-frequency component ($\Omega = 5$ in this case). This regime is depicted in Fig. 3(b), where it is compared with the above mentioned case where each spike follows the previous one almost periodically with the system internal frequency (Fig. 3(a)).

The VR effect illustrated in Fig. 2 can be quantified by computing the response Q of the system (i.e., the component from the Fourier spectrum) at the signal frequency ω, which is given by $Q = \sqrt{Q_{\sin}^2 + Q_{\cos}^2}$,

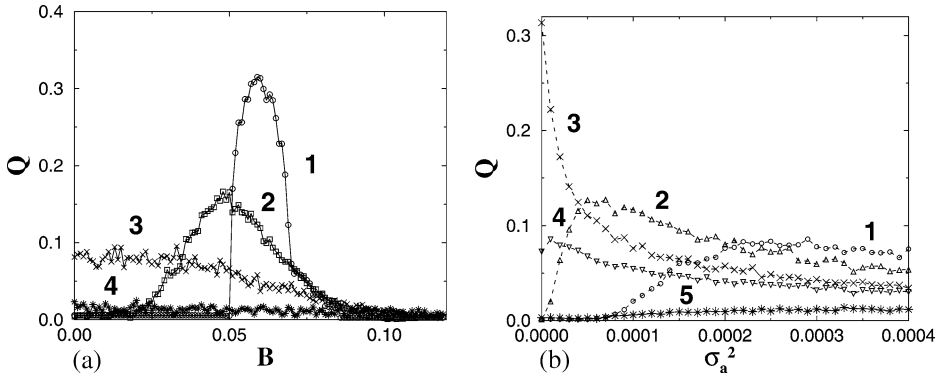

Fig. 4. Response of the system at the low frequency ω in the presence of additive noise: (a) versus the HF amplitude B for different intensities of additive noise (curve 1: $\sigma_a^2 = 0$, curve 2: $\sigma_a^2 = 0.05 \times 10^{-3}$, curve 3: $\sigma_a^2 = 0.25 \times 10^{-3}$, curve 4: $\sigma_a^2 = 3 \times 10^{-3}$; and (b) versus the noise intensity σ_a^2 for different amplitudes (curve 1: $B = 0$, curve 2: $B = 0.04$, curve 3: $B = 0.06$, curve 4: $B = 0.07$, curve 5: $B = 0.1$).

where

$$Q_{\sin} = \frac{\omega}{\pi n} \int_0^{2\pi n/\omega} y(t) \sin(\omega t)\, dt,$$

$$Q_{\cos} = \frac{\omega}{\pi n} \int_0^{2\pi n/\omega} y(t) \cos(\omega t)\, dt. \tag{3}$$

The dependence of this response on the amplitude of the high-frequency driving (Fig. 3(c)) displays a resonant form with a clearly defined maximum at $B \sim 0.06$, similarly to what happens in SR. The staircase form of this dependence is caused by the abrupt discrete appearance of new spikes in the spike train as the forcing amplitude increases. The staircase pattern persists (although its shape may change) when the frequency ratio between the two periodic signal changes, even when this ratio is incommensurate. We have checked that the resonance displayed in Fig. 3(c) persists for a wide range of values of the high-frequency around $\Omega = 5.0$ (the values tested cover the range 2.0–17.0). However, due to the additional interplay between the HF signal and sub-threshold oscillations, the position and amplitude of the resonance peak vary with the value of the high frequency. This behavior constitutes a difference with respect to the standard SR effect, and could be useful for determining the system's natural selectivity of special frequency components from the white noise when SR occurs.

So far we have not considered the influence of noise in the behavior of the FHN model. In order to study the interplay of VR and SR in this system, we now increase the intensity σ_a^2 of additive noise in the system. Fig. 4(a) shows that by adding noise to the system the response dependence is shifted to the left and decreased. Hence, with increasing noise the maximum of the response is achieved for a smaller value of B (compare curves 1 and 2 in Fig. 4(a)). This fact could be relevant for an efficient information processing, because natural fluctuations or noise (unavoidably present in experimental systems) are able to replace a fraction of the high-frequency driving and help to reduce the necessary input energy. If the noise intensity is too large, VR dissapears (curve 4 in Fig. 4(a)). Next we analyze the response of the system as a function of noise intensity for varying amplitude B of the HF forcing (see Fig. 4(b)). For no HF amplitude (curve 1 in the figure) standard SR is found. Adding then a high-frequency driving to the signal improves SR, because the resonance curve is shifted to lower values of σ_a^2 and is increased (curve 2 in Fig. 4(b)). Hence the amount of noise needed for an optimal signal processing is smaller. We can thus interpret that a high-frequency driving allows us to control stochastic resonance. Further increase of B to the value which corresponds to the optimal amplitude $B = 0.06$ in the noise-free case leads only to a monotonous decrease of the quality of signal processing with increasing noise intensity σ_a^2, shown as curve 3 in Fig. 4(b) (but its value at zero noise is the largest one among all curves, as expected from the optimal driving amplitude – compare the values at $\sigma_a^2 = 0$ of all the curves in Fig. 4(b) with curve 1 in Fig. 4(a)). For even larger values of B, signal

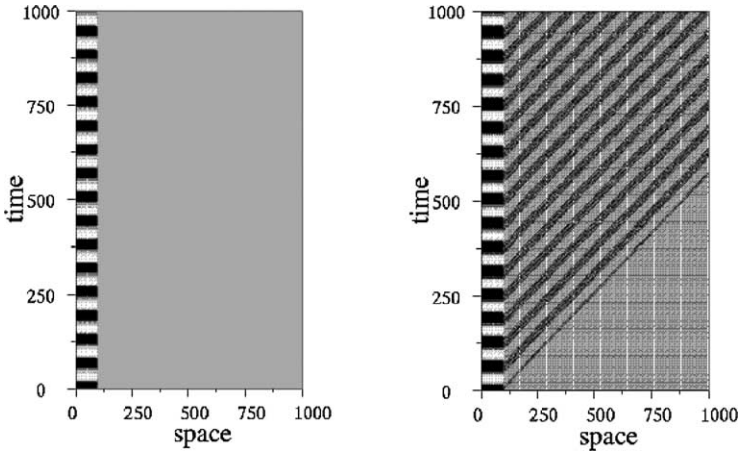

Fig. 5. Resonant vibrational propagation in a excitable medium. A chain of coupled oscillators (Eqs. (4)) is represented along the horizontal axis z. Time evolution goes from bottom to top. Left: without HF vibration ($B = 0$); right: with HF vibration ($B = 1.6$). The first 100 oscillators ($i < i_{\text{ex}}$) are always driven by the low-frequency signal. An increase of high-frequency vibration leads to propagation of the information LF signal.

processing has very bad quality for all intensities of additive noise (curves 4 and 5).

4. Resonant vibrational propagation

When excitable systems are coupled spatially in an extended medium, excitation pulses are able to propagate through the system in a very efficient way. Consequently, it is interesting to analyze whether the phenomenon of vibrational resonance can be generalized to the case of spatially extended systems. To that end we consider a chain of coupled excitable oscillators, whose behavior we represent now by the Barkley model [28]:

$$\begin{aligned}\frac{du_i}{dt} &= \frac{1}{\varepsilon}u_i(1-u_i)\left(u_i - \frac{v_i+b}{a}\right) \\ &\quad + \frac{D}{\Delta x}\sum_{j\in N(i)} c_{ij}u_j + A_i\cos(\omega t) + B\cos(\Omega t), \\ \frac{dv_i}{dt} &= cu_i - v_i, \end{aligned} \tag{4}$$

where i is the cell index along the chain, and we take $A_i = 0$ for $i > i_{\text{ex}}$. In what follows we used the following values for the model parameters: $\epsilon = 0.01$, $a = 0.85$, $b = 0.18$, and $c = 0.7$ (for which the system operates locally in an excitable regime) and the coupling strength is taken $D = 0.05$. The weight coefficients c_{ij} correspond to the first-order discretization of the Laplacian operator [29] with $\Delta x = 0.25$. Every oscillator in the chain is driven by a high-frequency signal $B\cos(\Omega t)$, with $\Omega = 5.0$, and the oscillators with $i < i_{\text{ex}}$ are additionally under the action of the low-frequency information-carrying signal $A\cos(\omega t)$, with $\omega = 0.1$ and $A = 3.0$.

The behavior of this extended system is illustrated in Fig. 5. When no high-frequency vibration ($B = 0$) is applied to the oscillators the signal is unable to propagate for the coupling strength chosen (Fig. 5 left). However, if we now apply a HF vibration ($B = 1.6$) to all oscillators in the chain, the LF information-carrying signal propagates through the whole chain of oscillators as a train of pulses (Fig. 5 right). The mechanism of this effect is based on the occurrence of VR in single oscillators, but now the input of each oscillator (for $i > i_{\text{ex}}$) comes from the output of the previous element in the chain. Hence, the effect of VR in excitable oscillators can be observed in spatially extended systems as a resonant *vibrational propagation*.

5. Conclusions

We have studied several aspects of the dynamical response of excitable systems to bichromatic signals with two very different frequencies. We have demon-

strated the existence of two phenomena: vibrational resonance in zero-dimensional systems and resonant vibrational propagation in spatially extended media. Experimental results obtained in an excitable electronic circuit have been confirmed by a numerical analysis of the FitzHugh–Nagumo model. In particular, it has been shown that an optimal amplitude of the high-frequency component of the signal can optimize signal processing of the low-frequency component, which encodes the information. We have also shown that in the presence of noise high-frequency driving can substitute a fraction of the noise and hence control the effect of stochastic resonance. In spatially extended excitable media, vibrational resonance enhances propagation of the low-frequency signal through the system by means of the action of the high-frequency driving. We have reported vibrational resonance and resonant vibrational propagation in simple systems and paradigmatic models, and have studied these effects in a general framework, hence we expect that these findings will be relevant for different fields, including communication technologies, optics, chemistry, neuroscience, and medicine. Given the ubiquity of two-frequency signals in neural systems, mentioned already in the introduction, this result could be of special interest in the study of the activity of neuron ensembles, and in general in wave propagation in excitable activatory–inhibitory systems.

Acknowledgements

A.Z. acknowledges financial support from CESCA-CEPBA through the EC IHP Program (HPRI-1999-CT-00071), and from the Microgravity Application Program/Biotechnology of the European Space Agency (ESA). J.G.O. was supported by the Ministerio de Ciencia y Tecnología (Spain, under projects BFM2001-2159 and BFM 2002-04369), E.U. by the International MP Research School on Biomimetic systems, and J.K. by SFB 555 (Germany).

References

[1] L. Gammaitoni, P. Hänggi, P. Jung, F. Marchesoni, Rev. Mod. Phys. 70 (1998) 223.
[2] R. Benzi, A. Sutera, A. Vulpiani, J. Phys. A 14 (1981) L453.
[3] B. McNamara, K. Wiesenfeld, R. Roy, Phys. Rev. Lett. 60 (1988) 2626.
[4] J. Douglass, L. Wilkens, L. Pantazelou, Nature 365 (1993) 337.
[5] K. Wiesenfeld, D. Pierson, E. Pantazelou, C. Dames, F. Moss, Phys. Rev. Lett. 72 (1994) 2125.
[6] S. Sinha, Physica A 270 (1999) 204.
[7] P. Landa, P. McClintock, J. Phys. A: Math. Gen. 33 (2000) L433.
[8] G.M. Shepherd, The Synaptic Organization of the Brain, Oxford Univ. Press, 1990.
[9] V. Mironov, V. Sokolov, Radiotekh. Electron. 41 (1996) 1501 (in Russian).
[10] D. Su, M. Chiu, C. Chen, Prec. Eng. 18 (1996) 161.
[11] A. Maksimov, Ultrasonics 35 (1997) 79.
[12] J. Victor, M. Conte, Visual Neurosci. 17 (2000) 959.
[13] V. Gherm, N. Zernov, B. Lundborg, A. Vastberg, J. Atmos. Solar–Terrestrial Phys. 59 (1997) 1831.
[14] C.W. Cho, Y. Liu, W.N. Cobb, T.K. Henthorn, K. Lillehei, U. Christians, K.Y. Ng, Pharm. Res. 19 (2002) 1123.
[15] J.L. Karnes, H.W. Burton, Arch. Phys. Med. Rehabil. 83 (2002) 1.
[16] O. Schlafer, T. Onyeche, H. Bormann, C. Schroder, M. Sievers, Ultrasonics 40 (2002) 25.
[17] R. Feng, Y. Zhao, C. Zhu, T.J. Mason, Ultrason. Sonochem. 9 (2002) 231.
[18] Y. Yu, W. Wang, J. Wang, F. Liu, Phys. Rev. E 63 (2001) 021907.
[19] P. Parmananda, H. Mahara, T. Amemiya, T. Yamaguchi, Phys. Rev. Lett. 87 (2001) 238302.
[20] S. Kádár, J. Wang, K. Showalter, Nature 391 (1998) 770;
J. García-Ojalvo, L. Schimansky-Geier, J. Stat. Phys. 101 (2000) 473;
J. García-Ojalvo, F. Sagués, J.M. Sancho, L. Schimansky-Geier, Phys. Rev. E 65 (2002) 011105.
[21] M. Löcher, D. Cigna, E.R. Hunt, Phys. Rev. Lett. 80 (1998) 5212;
J.F. Lindner, S. Chandramouli, A.R. Bulsara, M. Löcher, W.L. Ditto, Phys. Rev. Lett. 81 (1998) 5048;
J. García-Ojalvo, A.M. Lacasta, F. Sagués, J.M. Sancho, Europhys. Lett. 50 (2000) 427.
[22] A. Zaikin, J. García-Ojalvo, L. Schimansky-Geier, J. Kurths, Phys. Rev. Lett. 88 (2002) 010601.
[23] R. Báscones, J. García-Ojalvo, J.M. Sancho, Phys. Rev. E 65 (2002) 061108.
[24] J. Keener, J. Snyder, Mathematical Physiology, Springer, New York, 1998.
[25] A.S. Mikhailov, Foundations of Synergetics, 2nd Edition, Springer, Berlin, 1994.
[26] A. Pikovksy, J. Kurths, Phys. Rev. Lett. 78 (1997) 775.
[27] J. García-Ojalvo, J.M. Sancho, Noise in Spatially Extended Systems, Springer, New York, 1999.
[28] D. Barkley, M. Kness, L.S. Tuckerman, Phys. Rev. A 42 (1990) 2489.
[29] M. Abramowitz, I.A. Stegun, Handbook of Mathematical Functions, Dover, New York, 1972.